

Hydroclimate changes in eastern Africa over the past 200,000 years may have influenced early human dispersal

Frank Schaebitz^{1✉}, Asfawossen Asrat^{2,3}, Henry F. Lamb^{4,5}, Andrew S. Cohen⁶, Verena Foerster¹, Walter Duesing⁷, Stefanie Kaboth-Bahr⁷, Stephan Opitz⁸, Finn A. Viehberg⁹, Ralf Vogelsang¹⁰, Jonathan Dean¹¹, Melanie J. Leng¹², Annett Junginger¹³, Christopher Bronk Ramsey¹⁴, Melissa S. Chapot⁴, Alan Deino¹⁵, Christine S. Lane¹⁶, Helen M. Roberts⁴, Céline Vidal¹⁶, Ralph Tiedemann¹⁷ & Martin H. Trauth⁷

Reconstructions of climatic and environmental conditions can contribute to current debates about the factors that influenced early human dispersal within and beyond Africa. Here we analyse a 200,000-year multi-proxy paleoclimate record from Chew Bahir, a tectonic lake basin in the southern Ethiopian rift. Our record reveals two modes of climate change, both associated temporally and regionally with a specific type of human behavior. The first is a long-term trend towards greater aridity between 200,000 and 60,000 years ago, modulated by precession-driven wet-dry cycles. Here, more favorable wetter environmental conditions may have facilitated long-range human expansion into new territory, while less favorable dry periods may have led to spatial constriction and isolation of local human populations. The second mode of climate change observed since 60,000 years ago mimics millennial to centennial-scale Dansgaard-Oeschger cycles and Heinrich events. We hypothesize that human populations may have responded to these shorter climate fluctuations with local dispersal between montane and lowland habitats.

¹Institute of Geography Education, University of Cologne, Cologne, Germany. ²Department of Mining and Geological Engineering, Botswana University of Science and Technology, Palapye, Botswana. ³School of Earth Sciences, Addis Ababa University, Addis Ababa, Ethiopia. ⁴Department of Geography and Earth Sciences, Aberystwyth University, Aberystwyth, UK. ⁵Botany Department, School of Natural Sciences, Trinity College Dublin, Dublin, Ireland. ⁶Department of Geosciences, University of Arizona, Tucson, USA. ⁷Institute of Geosciences, University of Potsdam, Potsdam, Germany. ⁸Institute of Geography, University of Cologne, Cologne, Germany. ⁹Institute of Geography and Geology, University of Greifswald, Greifswald, Germany. ¹⁰Department of Prehistoric Archaeology, University of Cologne, Cologne, Germany. ¹¹Department of Geography, Geology and Environment, University of Hull, Hull, UK. ¹²British Geological Survey, Keyworth, UK and School of Biosciences, University of Nottingham, Nottingham, UK. ¹³Department of Geosciences, University of Tübingen, Tübingen, Germany. ¹⁴School of Archaeology, University of Oxford, Oxford, UK. ¹⁵Berkeley Geochronology Center, Berkeley, USA. ¹⁶Department of Geography, University of Cambridge, Cambridge, UK. ¹⁷Institute Biology and Biochemistry, University of Potsdam, Potsdam, Germany. ✉email: frank.schaebitz@uni-koeln.de

Reasons for the mobility and dispersal of *Homo sapiens* both within and out of Africa are still a matter of debate¹. Recent discoveries of human fossils and related stone tools between ~315 and 75 ka in age in several parts of Africa (e.g., northern Africa², southern Africa^{3,4}, and eastern Africa^{5,6}) have initiated a lively discussion of hypothesized multiregional origin and development of *Homo sapiens* within Africa⁷. This hypothesis includes a temporary availability of suitable, interconnected habitats, providing sufficient resources for our species to succeed and establish vital populations. Understanding human origins, refugia and dispersal is therefore dependent on accurate reconstructions of climatic and environmental conditions in time and space.

Today, the climate of eastern Africa is controlled by the annual migration of the tropical rain belt (TRB) following the zenith of the sun with a 3–4 week lag. This intensive insolation causes the build-up of mesoscale convective systems (MSCs), modulated by the possible influence of the West African (WAM) and South Asian (Indian) (SAM) monsoons, causing a unimodal to trimodal distribution of rainfall. On an interannual time scale, zonal atmospheric flow associated with the Walker Circulation (WC) and anomalies of the Indian Ocean sea-surface temperatures (SSTs) in combination with the Indian Ocean Dipole (IOD), modulate the intensity of the rainy seasons in eastern Africa^{8,9} (Supplementary Fig. S1). These controls are subject to orbital and millennial-to-centennial scale fluctuations, which have led to significant past fluctuations in regional precipitation and to habitat change, forcing the biota to adapt, migrate, or face local extinction^{10–14}.

Recently, geoscientists, climate experts, and paleoanthropologists have teamed up within the Hominin Sites and Paleolakes Drilling Project (HSPDP) to examine the relationship of human origin and climate change by drilling paleolake sequences near important hominin fossil and artifacts sites in the East African Rift^{15,16}. In addition, other studies of this region have investigated outcrops of lake sediment to reconstruct past climate variation and possible influences on human evolution, expansion, and technological innovation^{13,17}. These studies found that eastern African climate and environment have undergone repeated profound wet-dry transformations during the Quaternary, including the formation and disappearance of extensive lake systems accompanied by regional vegetation change. These transformations are often linked to orbitally-controlled insolation variations and millennial-to-centennial fluctuations associated with the high-latitude Dansgaard-Oeschger cycles (D/O) and Heinrich events (HEs)^{13,18–20}. In addition to climate change, lakes also fluctuate from non-climatic drivers, complicating reconstruction of climate fluctuations from these deposits¹³.

Using archives of environmental change to test established hypotheses of the evolution and expansion of *H. sapiens* is complicated by the potentially complex and non-deterministic response of humans to external natural factors²¹, which may vary due to social factors (i.e. relation to neighboring groups) and individual choices²². In addition, technological advances may have facilitated the ability of humans to cope with and adapt to climatic stress^{23,24}. The refugial hypothesis suggests that *H. sapiens* survived times of harsher living conditions, as small populations were able to move into more suitable environments with attendant consequences for genetic drift and natural selection²⁵. In eastern Africa, humans may have occupied mountain refugia along the rift margins^{26–28}.

To better understand the relationship between past climate change and the behavioral and migratorial response of *H. sapiens*, we reconstructed the last ~200 ka of eastern African climate change based on a sediment drill core collected in the Chew Bahir (CHB), a paleo-lake basin in southern Ethiopia (Fig. 1). Our

geochemical and sedimentological data set provides the first continuous climate record from southern Ethiopia covering the entire period of existence of *H. sapiens* in eastern Africa. Fossil evidence from the key paleoanthropological sites at Omo Kibish⁶ and Herto⁵ show that humans have occupied parts of Ethiopia during the last ~200,000 years. Our results can contribute to the current discussion regarding the effect of environmental conditions on the mobility and expansion of our species within and beyond Africa^{1,29,30}.

Results

The 292.87 m long composite sediment core from Chew Bahir covers the last 617 ka of environmental change in the southern Ethiopian rift. Based on our age model, the uppermost 99.3 mcd (meters composite depth) encompass the last ~200 ka^{31,32}. For this study, we have combined sedimentological and geochemical proxies of environmental change, including grain-size variability, X-ray fluorescence (XRF) scanning-based elemental ratios (K/Zr, Al/Si, Ca/Ti), as well as total organic carbon (TOC) and the oxygen isotope composition ($\delta^{18}\text{O}$) of endogenic calcite (Supplementary Figs. S2 and S3). Our results show that high amounts of coarser-grained sediments (core sections with >50% sand marked as gray bars in Supplementary Fig. S2) mostly coincide with lower K/Zr, higher Al/Si and Ca/Ti ratios, higher TOC, lower $\delta^{18}\text{O}$ values and vice versa.

Dry climate episodes at Chew Bahir, with increased evaporation, increased lake water alkalinity and salinity, and lowered lake levels have been inferred from the low-temperature illitisation of smectites in other cores from the site³³. During illitisation, also called reverse weathering process, which is initiated by increasing alkalinity and salinity in the pore water, Al-to-Mg substitutions lead to excess octahedral layer charge, which in turn enhances the K fixation in smectites³⁴. Hence, we interpret high K values as having developed during desiccation and low lake levels, similar to modern conditions.

Hydrologic-balance modeling shows that during the last wet phase, the so-called African Humid Period (AHP) at ~15–5 ka, with significantly lower K values, a precipitation increase of ~20–30% may have raised the Chew Bahir lake level by up to ~45 m compared to the present seasonally dry playa³⁵. Drier phases in the record are also generally characterized by an increase of silt-sized sediments, reduced chemical weathering (low Al/Si ratios), less organic matter accumulation reflected in lower TOC values, and higher $\delta^{18}\text{O}$ (Supplementary Fig. S3).

Changing Ca/Ti-ratios in the profile could be explained by processes dominating during contrasting hydrological conditions. For example, Ti may increase through fluvial input during wet episodes, or aeolian input during dry episodes. Additionally, the increased formation of authigenic carbonates in the sediment during dry phases could have raised Ca/Ti ratios while reduced carbonate production by organisms with calcareous shells during dry periods could have lowered them.

Clay-sized particles, indicative of deep lake conditions, are generally only a minor component of the sediment (a mean of ~3% of all grain size samples). However, sand layers often alternate with clay-rich beds (up to max. 39% clays) in the 61–100 mcd core interval (corresponding to ~200–125 ka; Supplementary Figs. S2 and S3). Silt-sized particles are much more abundant throughout the record (mean of 39%), but dominate (60–80%) in the uppermost 31 mcd (last ~60 ka). We interpret these medium-coarse silts to represent predominantly aeolian transport during more arid episodes.

Medium-grained sand layers are most common below 45 mcd (older than ~80 ka), indicative of more humid conditions when rivers were active and transporting coarser material. In addition,



Fig. 1 Location maps. **a** Map of Greenland and location of NGRIP ice core; **b** Map of northeastern Africa, the Near East, and southeastern Europe showing important fossil and archeological sites; **c** Map of northeastern Africa showing the location of the Chew Bahir drill site as well as important fossil and archeological sites. See text for details, data and references.

we argue that very fine silt and lacustrine clays were deposited during more humid periods when the precipitation/evaporation ratio was >1 , and a deep water body covered the sedimentary deposits for extended periods of time. Individual layers of very coarse sands are interpreted as reactivation products of the extensive alluvial fans at the western shores and surrounding ranges of the Chew Bahir basin, suggesting extreme rainfall events during a generally drier climate with reduced vegetation cover in the catchment³⁶.

Based on similar trends in our multi proxy data, namely the records of the K/Zr and Al/Si ratios, and the $\delta^{18}\text{O}$ values, we identify five distinct climate phases (Supplementary Fig. S3). The first wet phase (Phase I) between 200–125 ka was followed by Phase II which is characterized by a pronounced trend towards a drier, but also more variable climate from 125 to 60 ka. Thereafter, a dry phase (Phase III) between 60–14 ka can be observed in the K/Zr ratios and in the $\delta^{18}\text{O}$ values, which is succeeded by a wet phase (Phase IV; 14–5 ka) spanning the Early to Middle Holocene, which coincides with the well-established AHP (~15–5 ka)^{36–38}. During Phase V in the Late Holocene (between ~5–0 ka), the climate at Chew Bahir was persistently dry.

During Phases I and II (200–125 ka and 125–60 ka) we observe periodic alternations between wet and dry episodes on time scales of ~20 ka superimposed on the long-term drying trend. This relatively low frequency climate variability is superseded during the interval between 60–14 ka (Phase III) by repeated millennial-to-centennial scale abrupt shifts back to wetter climate conditions. Hence, we can distinguish between two distinct modes of climate change with low and high frequency climate variability at CHB, as can be seen particularly well in the K/Zr ratios, but also in other proxies such as Al/Si and Ca/Ti ratios. These observations are reiterated in the wavelet time-series analysis (Supplementary Fig. S4), which shows the strong influence of orbital precession between 200–125 ka, and which diminishes after about 80 ka, consistent with modeling results for the region¹⁸.

Discussion

We observe five climate phases including two modes of climate variability in the CHB during the last 200 ka (Supplementary Fig. S3). To explain this variability, we first compared our results to orbital eccentricity and precession (Fig. 2). Changes in these orbital parameters have been previously argued to be the dominant driver of eastern African climate variability^{21,39}. Phase I (200–125 ka) coincides with high eccentricity and strongly precession-dominated insolation changes, potentially driving the ~20 ka paced alternations between the well expressed wet and dry episodes during this time interval. In this scenario, precession minima/maxima, associated with high/low summer insolation led to a more/less northerly position of the African rainbelt, which could channel moisture towards CHB. The increased eccentricity thereby amplifies the effect of precession on the monsoonal changes and leads to either strongly expressed wet or dry episodes.

In contrast, during Phase II (125–60 ka), the gradual increase in aridity was accompanied by a lowering of the precession amplitude concurrent with decreasing eccentricity (Fig. 2; Supplementary Fig. S4). This reduced precessional amplitude led to an overall reduction in moisture transport towards CHB, causing a long-term drying trend. During Phase III (60–14 ka) eccentricity reaches its lowest value of the past 200 ka, with substantially subdued precessional amplitude and thus lower summer insolation. Consequently, the overall low insolation levels led to a contraction of the African rain belt and thus a precipitation focus south of the CHB watershed.

During Phase IV (14–5 ka) eccentricity increased again, associated with slightly wetter conditions before decreasing during Phase V (5 ka to present) in alignment with a drier climate. The close match between the hydroclimate at CHB and orbital eccentricity clearly demonstrates that orbital-scale insolation changes are the dominant driver of southern Ethiopian climate during the last 200 ka. We also find indications that periods with low insolation (low eccentricity) and reduced monsoonal impact may also be subject to a different climate driving mechanism, as suggested by the observed high-frequency climate variability during Phase III.

In the wider regional context, a comparison of the CHB record with the leaf-wax based vegetation and alkenone-based SST record from Gulf of Aden core RC09-166 suggests that during high eccentricity (Phase I; Marine Isotope Stage = MIS 7a to MIS 5e) the western Indian Ocean experienced a significant warming that decreased with decreasing eccentricity during Phase II and III (Fig. 2). As the Indian Ocean presents an important moisture source for eastern Africa today⁴⁰, arguably the warm SSTs during Phase I might have led to increased oceanic convection. When the African rain belt reached CHB during summer solstice (precession minimum), this increased oceanic convection may then have fueled the transport of moisture charged air masses to CHB. These findings underline the close link between hydroclimate in eastern Africa and Indian Ocean SSTs throughout the time covered by our core.

In contrast, the comparison between the CHB K/Zr ratio and the aridity indicated by the leaf wax proxy from the Gulf of Aden⁴¹ shows remarkable differences during Phase I (MIS 6; Fig. 2). In fact, the overall persistent humid conditions at CHB during this interval are seemingly opposite to persistent aridity in regions adjacent to the Gulf of Aden. The proposed aridity in this region seems peculiar as the neighboring Indian Ocean was relatively warm and should provide sufficient moisture for increased rainfall⁴¹. A possible explanation could be that convection-based precipitation during this period was more effective south of the Gulf and further inland. In this manner, the discrepancy in the moisture regime between CHB and the Gulf of Aden relates to changes in large-scale atmospheric circulation patterns⁴¹. Alternatively, it is possible that $\delta\text{D}_{\text{leaf wax}}$, which was used as the basis for the aridity proxy, records changes in moisture source rather than precipitation amount^{42,43}. Due to the contraction and widening of the tropical rain belt in correspondence with glacial-interglacial periods, it is possible that the moisture source changed⁴³ in the Gulf of Aden during Phase I (MIS 6).

Regional climate records from the African mainland support the humidity record from CHB. For example, the wet-dry index from an ocean core at ODP site 967 in the eastern Mediterranean Sea, which is a record of terrestrial dust flux and riverine inflow from the Nile river⁴⁴, parallels the CHB record. This is anticipated, since the upper Nile and Chew Bahir catchments are in close spatial proximity¹⁷, thus should record similar climate signals. The match between both proxy records and the sapropel layers emphasizes this tight coupling (Fig. 2) and suggests that increased humidity during Phase I at CHB was also reflected in the Nile River basin, hence into the Mediterranean realm.

Lake Tana, close to the source of the Blue Nile in northern Ethiopia, shows increased moisture availability at least during late Phase I, in line with CHB climate results⁴⁵. The repeated wet phases during Phase II (MIS 5e–5c) are also in agreement with wet phases inferred from the stalagmite record of the Mechara caves situated in the highlands northeast of the Chew Bahir basin⁴⁶ (Figs. 1 and 2). The authors also argue for a northern displacement of the African tropical rain belt caused by stronger summer insolation during times of stalagmite growth. The

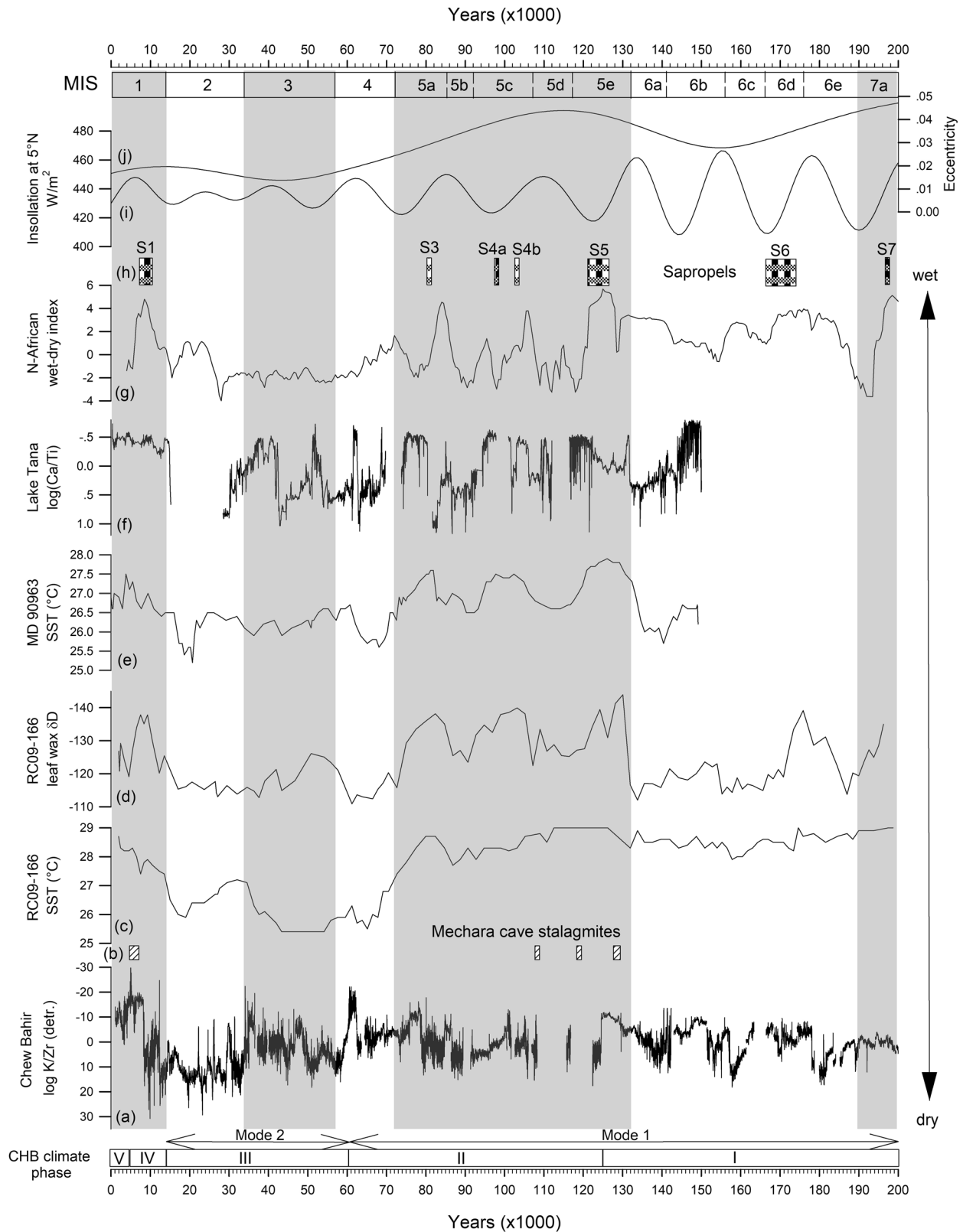


Fig. 2 Comparison of the log(K/Zr) record of the last 200 ka from the Chew Bahir basin (CHB) with other environmental records. a Detrended log(K/Zr) record from Chew Bahir; **b** Rectangles = Mechara cave stalagmite growth phases⁴⁶; **c** Alkenone-based SST and **d** Leaf wax based vegetation record from core RC09-166 from the Gulf of Aden⁴¹; **e** Indian Ocean sea-surface temperatures (SST)⁷⁰; **f** Detrended log(Ca/Ti) record from Lake Tana⁴⁵; **g** Wet-dry index from ODP 967⁴⁴; **h** Rectangles = sapropel layers⁵¹; **i** Insolation at 5°N and **j** Eccentricity variation⁷¹. Gray and white bars correspond to Marine Oxygen-Isotope Stages (MIS) according to⁷².

profound aridity during Phase III in Chew Bahir, at a time of reduced insolation levels, is also recorded in the Mediterranean realm and at Lake Tana from 60 to 55 ka, from 50 to 42 ka as well as after 35 ka⁴⁵.

The high-frequency climatic shifts during Phase III resemble northern hemisphere climate oscillations known as D/O cycles and HEs (Fig. 2 and Supplementary Fig. S5)^{19,20,47}. If the continental African site of CHB is indeed responding in phase with these oscillations, it suggests that at times of low eccentricity and hence diminished precessional amplitude, high-latitude processes increasingly influenced the climate at CHB. During HEs, the increased discharge of meltwater from the Northern Hemisphere ice cover led to a reduction of northward heat transport via the global oceanic conveyor belt⁴⁸. Consequently, heat and warm water accumulated in the tropics and subtropics of the southern hemisphere and the equatorial Atlantic, which led to a strong contraction or southward shift of the monsoonal rainbelt around the globe⁴⁹. This may have resulted in a reduction in monsoonal precipitation at CHB, thus explaining the observed millennial-scale dry spells coincident with HEs. The increased humidity during late Phase IV, corresponding to the AHP, is similar to the moisture variability during Phase I, in alignment with increased eccentricity and precession amplitude. The latter led to a more northward position of the African tropical rainbelt and thus increased humidity at CHB. The inferred moisture increase is again recorded at Lake Tana⁴⁵, the Mechara stalagmites⁴⁶ and the Mediterranean realm⁴⁴.

The significant precipitation changes inferred from the Chew Bahir record would have had a decisive influence on the living conditions of *H. sapiens* present in eastern Africa for at least the last 200 ka. Those profound transformations of the habitat of *H. sapiens* would have required adaptations in behavior or cultural development. The humid conditions observed in the oldest parts of the CHB record presented here (Fig. 3) coincide with the earliest *H. sapiens* fossils recovered to date in eastern Africa at ~195 ka, at Omo Kibish (~430 m asl), 90 km west of the Chew Bahir basin⁶. During this wettest episode of the record (~200–125 ka), with at least 20–30% more precipitation compared to today³⁵, extensive lakes and connected hydrological networks developed along the East African Rift System (EARS). This may have facilitated the long-distance movement of early modern humans, gathering food and finding sufficient water nearly everywhere in the lowlands of southern Ethiopia and the adjacent regions.

Between 200–190 ka and 185–170 ka, wetter conditions, and thus an expansion of favorable living conditions in large parts of northern and northeastern Africa and the Arabian Peninsula, are suggested by sapropel S7 and S6 at ODP site 967 in the Mediterranean Sea^{44,50,51}. This time interval also coincides with the first documented appearance of modern humans in the Levant, at Misliya Cave, with fossils dated at 194–177 ka²⁹. We therefore suggest that regions with favorable conditions were episodically connected from southern Ethiopia as far north as the Levant, opening early dispersal routes for *H. sapiens* out of eastern Africa⁵² as early as MIS 7a and during some intervals of MIS 6 (Fig. 3). The alignment between wet phases in the CHB record and other paleoclimate records to the NE⁴⁴ suggest that these favorable living conditions existed at multiple times not only in the lowlands of eastern Africa but also along the course of the Nile River, providing a pathway for early modern humans to move north.

Pronounced wet conditions were also prevalent during MIS 5e and 5c (Fig. 2) in the highlands northeast of the Chew Bahir basin, as interpreted from the stalagmite $\delta^{18}\text{O}$ record from the Mechara caves⁴⁶, implying favorable living conditions for humans over nearly all of northeastern Africa. Modern human

fossils have been recovered in northeastern Africa and the Levant that date back to these times^{4,5}. Moreover, human occupation layers in the Sodmein cave in the Eastern Egypt desert⁵³ and artefacts and human fossils from Al Wusta in Saudi Arabia⁵⁴, Skhul and Quafzeh⁵⁵ as well as human footprints in ancient lake sediments⁵⁶ also fall into MIS 5. These time windows have also been proposed by population modelers as possible episodes for early modern human expansion⁵⁷ (Fig. 3).

Genetic evidence points to the interval 70–60 ka for the most recent common ancestor (TMRCA) of mitochondrial haplogroup L3 from eastern Africa⁵⁸, fitting reasonably well to the subsequent 60–50 ka interval proposed as the oldest genetically based interval for dispersal from Africa of *H. sapiens* carrying L3 subtypes^{59,60}. The genetic time frame of 70–50 ka for “last long-range dispersal” coincides both with a more arid phase at CHB and overlaps with only a brief pronounced return to humidity in eastern Africa (60–62 ka, Fig. 3). This wet event may have offered a sufficiently long interval of suitable habitat in the lowlands of the EARS to facilitate dispersal of our species¹⁶.

The pronounced high-frequency climate fluctuations since ~60 ka, modulating the predominant trend towards an increasingly drier climate, could have repeatedly pushed *H. sapiens* populations to respond to the decrease of available surface water and food resources. These abrupt and frequent fluctuations may have exerted a level of climatic stress on humans that prompted new coping strategies and technological innovation, possibly reflected in the transition from Middle Stone Age (MSA) to late Stone Age (LSA) tool assemblages²². In addition, during this interval, *H. sapiens* employed other strategies to respond to environmental boundary conditions in the rift system: groups moved up to the Ethiopian highlands on both sides of the rift, as cave archeological records at Goda Buticha⁶¹, Mochena Borago^{26,62}, Fincha Habera²⁸, and Sodicho⁶³ suggest (Fig. 3).

Although chronological uncertainties in these records including CHB do not allow a precise comparison, the timing of the driest episodes in the CHB record generally agree with those of the highland occupations by *H. sapiens*. Settlement in higher-elevation sites persisted longer, encompassing the intervening short wet phases. The paucity of archeological and fossil records older than ~80 ka on the Ethiopian highlands limits our ability to test the refugia hypothesis during 80–200 ka. However, the oldest known high-elevation archeological site in the region shows evidence of Acheulian-aged occupation at Dendi volcano⁶⁴ (Fig. 1) in the northwestern Ethiopian highlands. This underscores that high mountain areas have long been tapped as favorable habitats by hominins.

This strategy of orographic mobility has been previously discussed in more detail for the much wetter southwestern Ethiopian highlands for several dry pulses during the youngest (15–5 ka) AHP²⁷. Generally, these findings support the idea that *H. sapiens* sought refuge at higher elevations as a potential coping strategy for fading resources and increasingly precarious living conditions in the rift valley. Thus, living in higher altitude zones could have been a climatically-triggered response to millennial scale droughts in the EARS. However, during the very dry Last Glacial Maximum (~20 ka), the highlands of Ethiopia seem to have remained largely unpopulated, possibly due to reaching an environmental threshold²⁷.

Documented wet phases at CHB, comparable to other sedimentological records of northeastern Africa during the last 200–60 ka, indicate recurrent availability of favorable living conditions in the lowlands of the EARS and adjacent regions for *H. sapiens*, which would have provided opportune corridors for our species to disperse into the Levant and Arabia. Increasing aridity in the lowlands of the southern Ethiopian rift valley starting during MIS 4 and intensifying aridity since 60 ka may

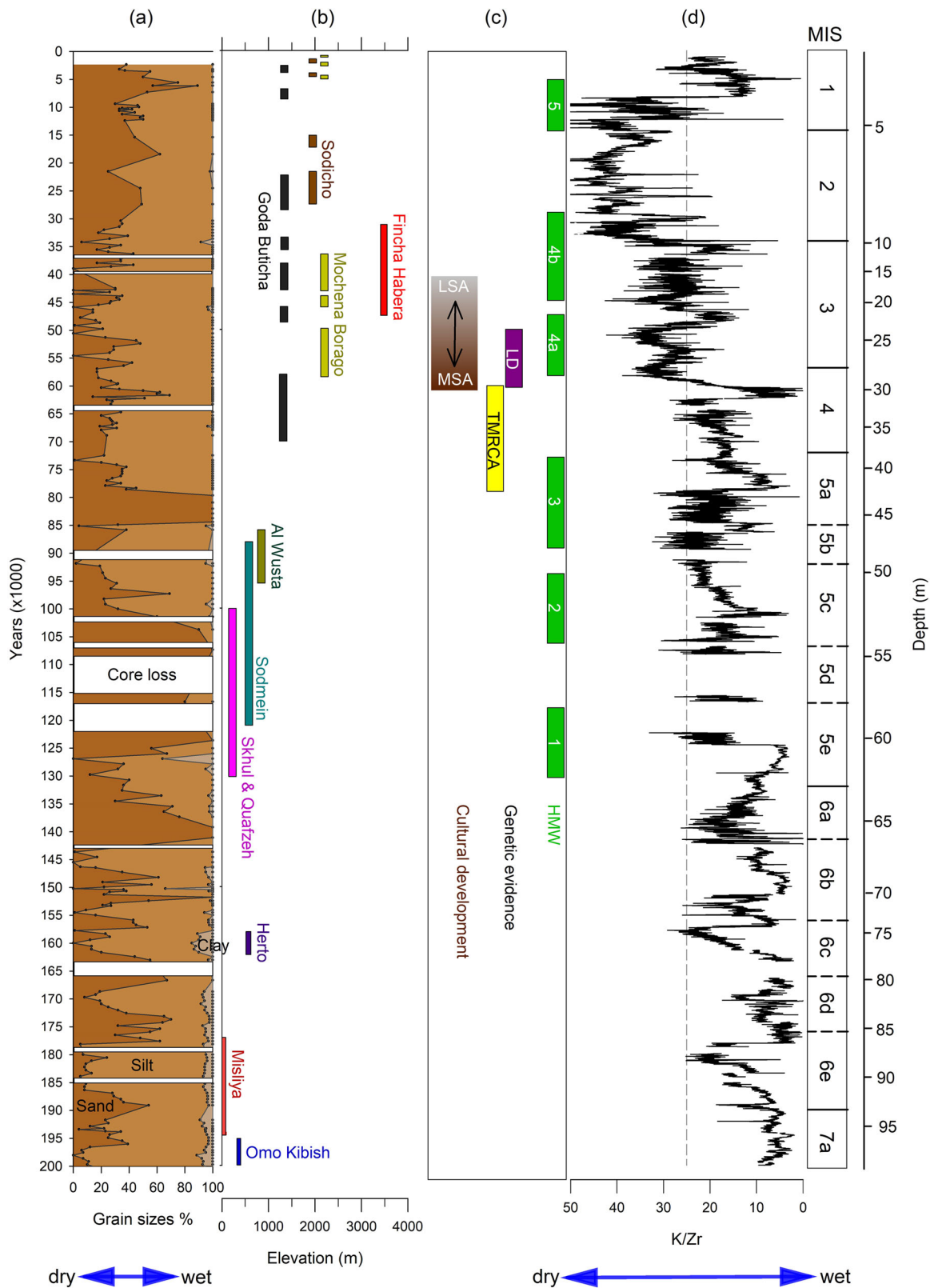


Fig. 3 Environmental record of the last 200 ka from the Chew Bahir basin (CHB). **a** Grain size distribution; **b** Chronological range of archeological/fossil sites with corresponding elevation of sites (for archeological/fossil sites location, see Fig. 1; for references see text); **c** Modeled Human Migration Windows (HMW = green rectangles)⁵⁷, genetic evidence (TMRCA = time to most recent common ancestor⁵⁸ and LD = last dispersal of *Homo sapiens*^{59, 60}); **d** Record of K/Zr ratio from the Chew Bahir basin; Marine Oxygen-Isotope Stages (MIS) according to⁷².

have induced *H. sapiens* to develop, test and use new strategies to survive, including occupation of high mountain refugia and the development of new tools.

Methods

During the CHB deep drilling campaign in Nov. 2014, two sediment cores were recovered: HSPDP-CHB14-2A and -2B (Fig. 1; N 4.7612° E 36.7668° and N 4.7613° E 36.7670°; 500 m asl) reaching down to 278.58 mbs (= meters below surface) and 266.38 mbs, respectively¹⁵. The cores were collected ~20 m apart and a composite record of 292.87 mcd (= meters composite depth) was constructed using a multi-parameter approach^{31,32}. Technical difficulties during coring through sand layers (Supplementary Fig. S2; white bars in the grainsize column) led to some core loss at ~78–80, 58–59 and 55–57 mcd, and to a lesser extent also at 13, 15.5, 33.5, 49, 87.5 and 90.5 mcd. Core recovery rate in the upper 100 m is ~89.5%.

A total of 743 discrete samples collected every ~32 cm through the whole core were analyzed for their particle size distribution, 250 samples from 0.6 to 99.2 m depth represent the uppermost 200 ka. Prior to grainsize measurements the organic and carbonate components were removed. For this purpose, the samples (fine-grained fraction, <2 mm) were pretreated with H₂O₂ (30%) and with 15% HCl. For the final aggregate dispersion 0.5 N Na₂P₂O₇ (55.7 g/l) was added. The particle size distribution of each sample was measured three times with a Beckman Coulter LS 13320 laser particle analyzer with 116 particle size classes from 0.04–2000 µm using the Fraunhofer optical model. The calculation of the univariate statistical particle size values was performed with the software GRADISTAT⁶⁵.

Elemental variations were determined by X-ray fluorescence (XRF) core scanning at 5 mm resolution along the CHB composite profile with an Itrax core scanner at the Large Lakes Observatory (LLO) of the University of Minnesota Duluth. Following HSPDP protocols, a Chromium (Cr) tube was used with a tube voltage of 30 kV, current of 30 mA and scanning time of 10 s⁶⁶. All XRF data were normalized by dividing elemental counts by coherence scattering and multiplied by a correction factor to compensate for e.g. the aging of the Cr tube. Subsequently, all data sets have been cleaned sub-cm wise to avoid coring artifacts such as cracks and voids^{32,67}. According to the age model, the 5 mm spacing of the XRF data corresponds to ~10 years³¹. High K values have been established as an aridity proxy for paleolake Chew Bahir, controlled by increasing pore water alkalinity under dry conditions^{16,32,33}. The XRF K values are normalized with Zr as a proxy for detrital influx into the lake. For better comparison to other records we also used the log K/Zr (detrended) values.

High Al/Si ratios are interpreted as indicator for the intensity of chemical weathering of feldspars, micas, amphiboles and pyroxenes in the catchment under generally wetter conditions that showed more uniformly distributed rainfall. Ca/Ti is used as a proxy for both biogenic calcite production in the water column and precipitation of authigenic calcite in the sediment, normalized for Ti as a proxy of the influx of clastic material into the lake⁶⁸.

The concentration of total carbon (TC) was measured in a total of 842 samples (32 cm intervals; 239 samples represent the uppermost ~200 ka) with a non-dispersive infrared sensor (Dimatec Ltd.) to analyze the thermic-catalytic oxidation process for both total inorganic carbon (TIC) and total carbon. To determine the content of total organic carbon (TOC), the difference between TC and TIC was calculated. Higher TOC values indicate more organic material in the sediments due to higher production in wetter climate conditions. An elemental analyzer (vario MICRO cube, Elementar Ltd.) was used to verify the TC values. Where reproduced values differed by > 5% samples were remeasured.

Excluding calcite nodules and dolomite in the bulk sediment samples, the δ¹⁸O composition of bleached endogenic calcite was analyzed using a Thermo Finnigan MAT 253 mass spectrometer at the British Geological Survey, UK, following standard vacuum techniques⁶⁹. Data are given as per mil (‰) deviations from the VPDB standard. Based on standard materials, analytical reproducibility was < 0.1‰. Lower δ¹⁸O values indicate wetter conditions. 152 δ¹⁸O samples represent the uppermost ~200 ka of the CHB record.

Prior to time-series analysis, the data were interpolated to an evenly-spaced time axis with 0.012 ka resolution. We calculate a continuous wavelet transformation (CWT) from the log(K/Zr) record using the MATLAB function *cwt*. We chose *Morlet* as the mother wavelet, which is very well suited to reproduce the cyclical characteristics of environmental variability in the Chew Bahir record.

Data availability

The proxy data of CHB is available online for download at LacCore Institute (Minneapolis USA, <http://lrc.geo.umn.edu/laccore/>; <https://doi.org/10.17605/OSF.IO/M8QU5>) and at the Collaborative Research Centre 806 Database (Cologne, Germany: <http://www.crc806db.uni-koeln.de>; <https://doi.org/10.5880/SFB806.66>).

Code availability

The script to compute the wavelet power spectrum will be made available through the MRES blog of M.H. Trauth, hosted at the University of Potsdam (<http://mres.uni-potsdam.de>).

Received: 19 October 2020; Accepted: 19 May 2021;

Published online: 14 June 2021

References

- Scerri, E. M. L., Chikhi, L. & Thomas, M. G. Beyond multiregional and simple out-of-Africa models of human evolution. *Nat Ecol Evol* **3**, 1370–1372 (2019).
- Hublin, J. J. et al. New fossils from Jebel Irhoud, Morocco and the pan-African origin of *Homo sapiens*. *Nature* **546**, 289–292 (2017).
- Grün, R. et al. Direct dating of Florisbad hominid. *Nature* **382**, 500–501 (1996).
- Stringer, C. The origin and evolution of *Homo sapiens*. *Philos. Trans. R. Soc. B: Biol. Sci.* **371**, 20150237 (2016).
- White, T. D., Asfaw, B., DeGusta, D. & Gilbert, H. Pleistocene *Homo sapiens* from Middle Awash, Ethiopia. *Nature* **423**, 742–747 (2003).
- Aubert, M. et al. Confirmation of a late middle Pleistocene age for the Omo Kibish 1 cranium by direct uranium-series dating. *J Hum Evol* **63**, 704–710 (2012).
- Scerri, E. M. L. et al. Did Our Species Evolve in Subdivided Populations across Africa, and Why Does It Matter? *Trends Ecol Evol* **33**, 582–594 (2018).
- Saji, N. H., Goswami, B. N., Vinayachandran, P. N. & Yamagata, T. A dipole mode in the tropical Indian Ocean. *Nature* **401**, 360 (1999).
- Nicholson, S. E. An analysis of recent rainfall conditions in eastern Africa. *International Journal of Climatology* **36**, 526–532 (2016).
- Raia, P. et al. Past Extinctions of Homo Species Coincided with Increased Vulnerability to Climatic Change. *One Earth* **3**, 480–490 (2020).
- Tryon, C. A. The Middle/Later Stone Age transition and cultural dynamics of late Pleistocene East Africa. *Evol Anthropol* **28**, 267–282 (2019).
- Mirazón Lahr, M. The shaping of human diversity: filters, boundaries and transitions. *Philos Trans R Soc Lond B Biol Sci* **371**, (2016).
- Trauth, M. H., Maslin, M. A. & Strecker, M. R. Late Cenozoic Moisture History of East Africa. *Science* **309**, 2051–2053 (2005).
- Trauth, M. H. et al. Human evolution in a variable environment: the amplifier lakes of Eastern Africa. *Quaternary Science Reviews* **29**, 2981–2988 (2010).
- Cohen, A. et al. The Hominin Sites and Paleolakes Drilling Project: inferring the environmental context of human evolution from eastern African rift lake deposits. *Sci. Drill.* **21**, 1–16 (2016).
- Viehberg, F. A. et al. Environmental change during MIS4 and MIS 3 opened corridors in the Horn of Africa for *Homo sapiens* expansion. *Quaternary Science Reviews* **202**, 139–153 (2018).
- Junginger, A. & Trauth, M. H. Hydrological constraints of paleo-Lake Suguta in the Northern Kenya Rift during the African Humid Period (15–5 ka BP). *Global and Planetary Change* **111**, (2013).
- Kutzbach, J. E. & Street-Perrott, F. A. Milankovitch forcing of fluctuations in the level of tropical lakes from 18 to 0 kyr BP. *Nature* **317**, 130–134 (1985).
- Stager, J. C., Mayewski, P. A. & Meeker, L. D. Cooling cycles, Heinrich event 1, and the desiccation of Lake Victoria. *Palaeogeography, Palaeoclimatology, Palaeoecology* **183**, 169–178 (2002).
- Tierney, J. E. et al. Northern hemisphere controls on tropical southeast African climate during the past 60,000 years. *Science* **322**, 252–255 (2008).
- Maslin, M. A., Trauth, M. H. in *The first Humans - Origin and Early Evolution of the Genus Homo* (eds Grine, F. E., Fleagle, J. G. & Leakey, R. E.) 151–158 (Springer, 2009).
- Blinkhorn, J. & Grove, M. The structure of the Middle Stone Age of eastern Africa. *Quaternary Science Reviews* **195**, 1–20 (2018).
- Hoffecker, J. F. & Hoffecker, I. T. Technological complexity and the global dispersal of modern humans. *Evolutionary Anthropology: Issues, News, and Reviews* **26**, 285–299 (2017).
- Potts, R. et al. Environmental dynamics during the onset of the Middle Stone Age in eastern Africa. *Science* **360**, 86–90 (2018).
- Stewart, J. R. & Stringer, C. B. Human evolution out of Africa: the role of refugia and climate change. *Science* **335**, 1317–1321 (2012).
- Brandt, S., Hildebrand, E., Vogelsang, R., Wolfhagen, J. & Wang, H. A new MIS 3 radiocarbon chronology for Mochena Borago Rockshelter, SW Ethiopia: Implications for the interpretation of Late Pleistocene chronostratigraphy and human behavior. *Journal of Archaeological Science: Reports* **11**, 352–369 (2017).
- Foerster, V. et al. Environmental change and human occupation of southern Ethiopia and northern Kenya during the last 20,000 years. *Quaternary Science Reviews* **129**, 333–340 (2015).
- Ossendorf, G. et al. Middle Stone Age foragers resided in high elevations of the glaciated Bale Mountains, Ethiopia. *Science* **365**, 583–587 (2019).
- Hershkovitz, I. et al. The earliest modern humans outside Africa. *Science* **359**, 456–459 (2018).

30. Petraglia, M. D., Breeze, P. S. & Groucutt, H. S. in *Geological Setting, Palaeoenvironment and Archaeology of the Red Sea 675–683* (Springer International Publishing, Cham, 2019).
31. Roberts, H. M. et al. Using multiple chronometers to establish a long, directly-dated lacustrine record: constraining >600,000 years of environmental change at Chew Bahir, Ethiopia. *QSR* (in review).
32. Foerster, V. et al. 620,000 years of eastern Africa climate variability and hominin evolution. *Nature Geoscience* (in review).
33. Foerster, V. et al. Towards an understanding of climate proxy formation in the Chew Bahir basin, southern Ethiopian Rift. *Palaeogeography, Palaeoclimatology, Palaeoecology* **501**, 111–123 (2018).
34. Arnold, G. E., et al. Advanced hyperspectral analysis of sediment core samples from Chew Bahir Basin, Ethiopian Rift in the spectral range from 0.25 to 17 μm : support for climate proxy information. *Frontiers in Earth Sciences Spec. Iss.*, (accepted).
35. Fischer, M. L. et al. Determining the Pace and Magnitude of Lake Level Changes in Southern Ethiopia Over the Last 20,000 Years Using Lake Balance Modeling and SEBAL. *Frontiers in Earth Science* **8**, (2020).
36. Foerster, V. et al. Climatic change recorded in the sediments of the Chew Bahir basin, southern Ethiopia, during the last 45,000 years. *Quaternary International* **274**, 25–37 (2012).
37. Beck, C. C., Feibel, C. S., Wright, J. D. & Mortlock, R. A. Onset of the African Humid Period by 13.9 kyr BP at Kabua Gorge, Turkana Basin, Kenya. *The Holocene* 0959683619831415 (2019).
38. Castañeda, I. S. et al. Hydroclimate variability in the Nile River Basin during the past 28,000 years. *Earth and Planetary Science Letters* **438**, 47–56 (2016).
39. Trauth, M. H., Larrasoana, J. C. & Mudelsee, M. Trends, rhythms and events in Plio-Pleistocene African climate. *Quaternary Science Reviews* **28**, 399–411 (2009).
40. Nicholson, S. E. Climate and climatic variability of rainfall over eastern Africa: Climate Over Eastern Africa. *Rev. Geophys.* **55**, 590–635 (2017).
41. Tierney, J. E., deMenocal, P. B. & Zander, P. D. A climatic context for the out-of-Africa migration. *Geology* **45**, 1023–1026 (2017).
42. Wu, H., Zhang, X., Xiaoyan, L., Li, G. & Huang, Y. Seasonal variations of deuterium and oxygen-18 isotopes and their response to moisture source for precipitation events in the subtropical monsoon region. *Hydrological Processes* **29**, 90–102 (2015).
43. Levin, N. E., Zipser, E. J. & Cerling, T. E. Isotopic composition of waters from Ethiopia and Kenya: Insights into moisture sources for eastern Africa. *Journal of Geophysical Research* **114**, 1–13 (2009).
44. Grant, K. M. et al. A 3 million year index for North African humidity/aridity and the implication of potential pan-African Humid periods. *Quaternary Science Reviews* **171**, 100–118 (2017).
45. Lamb, H. F. et al. 150,000-year palaeoclimate record from northern Ethiopia supports early, multiple dispersals of modern humans from Africa. *Sci Rep* **8**, 1077 (2018).
46. Asrat, A. et al. Paleoclimate change in Ethiopia around the last interglacial derived from annually-resolved stalagmite evidence. *Quaternary Science Reviews* 1–14 (2018).
47. Andersen, K. K. et al. High-resolution record of Northern Hemisphere climate extending into the last interglacial period. *Nature* **431**, 147–151 (2004).
48. Böhm, E. et al. Strong and deep Atlantic meridional overturning circulation during the last glacial cycle. *Nature* **517**, 73–76 (2015).
49. Schmidt, M. W., Vautravers, M. J. & Spero, H. J. Rapid subtropical North Atlantic salinity oscillations across Dansgaard-Oeschger cycles. *Nature* **443**, 561–564 (2006).
50. Löwemark, L. et al. Sapropel burn-down and ichnological response to late Quaternary sapropel formation in two ~400 kyr records from the eastern Mediterranean Sea. *Palaeogeography, Palaeoclimatology, Palaeoecology* **239**, 406–425 (2006).
51. Ehrmann, W., Schmiedl, G., Beuscher, S. & Krüger, S. Intensity of African Humid Periods Estimated from Saharan Dust Fluxes. *PLoS One* **12**, e0170989 (2017).
52. deMenocal, P. B. & Stringer, C. Human migration: Climate and the peopling of the world. *Nature* **538**, 49–50 (2016).
53. Schmidt, C., Kindermann, K., van Peer, P. & Bubenzer, O. Multi-emission luminescence dating of heated chert from the Middle Stone Age sequence at Sodmein Cave (Red Sea Mountains, Egypt). *J. Archaeol. Sci.* **63**, 94–103 (2015).
54. Groucutt, H. S. et al. *Homo sapiens* in Arabia by 85,000 years ago. *Nat Ecol Evol* **2**, 800–809 (2018).
55. Grün, R. et al. U-series and ESR analyses of bones and teeth relating to the human burials from Skhul. *J. Human Evol.* **49**, 316–334 (2005).
56. Stewart, M. et al. Human footprints provide snapshot of last interglacial evolution in the Arabian interior. *Sci Adv* **6**, eaba8940 (2020). 1–10.
57. Timmermann, A. & Friedrich, T. Late Pleistocene climate drivers of early human migration. *Nature* **538**, 92–95 (2016).
58. Soares, P. et al. The expansion of mtDNA Haplogroup L3 within and out of Africa. *Mol Biol Evol* **29**, 915–927 (2012).
59. Mellars, P., Gori, K. C., Carr, M., Soares, P. A. & Richards, M. B. Genetic and archaeological perspectives on the initial modern human colonization of southern Asia. *Proc Natl Acad Sci USA* **110**, 10699–10704 (2013).
60. Mallick, S. et al. The Simons Genome Diversity Project: 300 genomes from 142 diverse populations. *Nature* **538**, 201–206 (2016).
61. Tribolo, C. et al. Across the gap: geochronological and sedimentological analyses from the late pleistocene-holocene sequence of Goda Buticha, Southeastern Ethiopia. *PLoS ONE* **12**, e0169418 (2017).
62. Vogelsang, R. & Wendt, K. P. Reconstructing prehistoric settlement models and land use patterns on Mt. Damota/SW Ethiopia. *Quaternary International* **485**, 140–149 (2018).
63. Hensel, E. A., Vogelsang, R., Noack, T. & Bubenzer, O. Stratigraphy and Chronology of Sodicho Rockshelter – A New Sedimentological Record of Past Environmental Changes and Human Settlement Phases in Southwestern Ethiopia. *Front. Earth Sci.* **8**, 611700, <https://doi.org/10.3389/feart.2020.611700> (2021).
64. Vogelsang, R. et al. When Hominins Conquered Highlands—an Acheulean Site at 3000 m a.s.l. on Mount Dendi/Ethiopia. *J. Paleo. Arch.* **1**, 302–313 <https://doi.org/10.1007/s41982-018-0015-9> (2018).
65. Blott, S. J. & Pye, K. GRADISTAT: a grain size distribution and statistics package for the analysis of unconsolidated sediments. *Earth Surface Processes Landforms* **26**, 1237–1248 (2001).
66. Campisano, C. J. et al. The hominin sites and paleolakes drilling project: high-resolution paleoclimate records from the east African rift system and their implications for understanding the environmental context of hominin evolution. *PaleoAnthropology* 1–43 (2017).
67. Trauth, M. H. et al. Classifying past climate change in the Chew Bahir basin, southern Ethiopia, using recurrence quantification analysis. *Climate Dynamics* **53**, 2557–2572 (2019).
68. Croudace, I. W. & Rothwell, R. G. *Micro-XRF Studies of Sediment Cores: Applications of a non-destructive tool for the environmental sciences* (Springer, 2015).
69. Dean, J. R. et al. Eastern Mediterranean hydroclimate over the late glacial and Holocene, reconstructed from the sediments of Nar lake, central Turkey, using stable isotopes and carbonate mineralogy. *Quaternary Sci. Rev.* **124**, 162–174 (2015).
70. Bard, E., Rostek, F. & Sonzogni, C. Interhemispheric synchrony of the last deglaciation inferred from alkenone palaeothermometry. *Nature* **385**, 707 (1997).
71. Laskar, J. et al. A long-term numerical solution for the insolation quantities of the Earth. *Astronom. Astrophys.* **428**, 261–285 (2004).
72. Railsback, L. B., Gibbard, P. L., Head, M. J., Voarintsoa, N. R. G. & Toucanne, S. An optimized scheme of lettered marine isotope substages for the last 1.0 million years, and the climatostratigraphic nature of isotope stages and substages. *Quaternary Sci. Rev.* **111**, 94–106 (2015).

Acknowledgements

Support for HSPDP was provided by the National Science Foundation (EAR-1338553) and the International Continental Drilling Program (ICDP). Chew Bahir drilling was supported by Deutsche Forschungsgemeinschaft (DFG, German Research Foundation) through the Priority Program SPP 1006 ICDP (FS: SCHA 472/13 and /18, MHT: TR 419/8, /10 and /16) and the Collaborative Research Center (CRC) 806 “Our Way to Europe”, Project Number 57444011. Support has also been received from the UK Natural Environment Research Council (NERC, NE/K014560/1, IP/1623/0516). Geochronological research was supported by National Science Foundation grant EAR 1322017 to AD. We thank the Federal and Regional Governments of Ethiopia, and the Hammar woreda local authorities for providing drilling permit and facilitating drilling activities in the Chew Bahir basin. The Ministry of Mines of Ethiopia is acknowledged for permitting and facilitating sample exports. We thank DOSECC Exploration Services for drilling supervision, EthioDer pvt. Ltd. Co. for providing logistical support during the drilling operations. We would like to extend our gratitude for the unreserved support we received from the Hammar people and the Turmi Police Administration during the whole period of the drilling operations. Initial core processing and sampling were conducted at the US National Lacustrine Core Facility (LacCore) at the University of Minnesota. We would also like to thank the Hammar elder chief Weino, Mesfin Mekonnen, Jonas Urban, Gerrit Dorenbeck, Bahru Zinaye Asegahegn, Meklit Yadeta, Christian Mast, Steve Cole, Antoni J. Vecchiarelli, Beau Marshall, Ryan O’Grady, Jessica Rodysill, Kristina Brady Shannon, Dorothea Klinghardt, Nicole Mantke, Erik Brown, Mona Stockhecke and Sinja Kraus, for their support during drilling and laboratory work. Thanks go to Frederik von Reumont for creating Fig. 1 and Daniel Gebregiorgis for editing Supplementary Fig. S2 of this paper. S.K.B. has received additional financial support from the University of Potsdam Open Topic Postdoc Program. This is publication No. 37 of the Hominin Sites and Paleolakes Drilling Project.

Author contributions

A.A., A.C., H.L., F.S., and M.H.T. initiated the Chew Bahir Drilling Project (CBDP) as part of the Hominin Sites and Paleolakes Drilling Project (HSPDP) and the A3-project of CRC 806 organized & guided by F.S.; field work and coring was led by A.A. & F.S. and assisted by V.F., A.J.; V.F. F.S. and M.H.T. designed the study that led to this manuscript; chronology data were generated by H.M.R. and M.S.C. (OSL), C.B.R. (^{14}C), A.D. ($^{40}\text{Ar}/^{39}\text{Ar}$), C.S.L. and C.V. (tephrochronology), and H.M.R. and C.B.R. created the age model; quantitative XRF analysis was done by V.F.; F.A.V. contributed to the general discussion and provided TC, TIC and TOC data; J.D. performed the oxygen isotope measurements in collaboration with M.J.L.; S.O. & F.S. performed the grainsize analysis; hydrology and micro-paleontological interpretation was done by A.J.; proxy interpretation and discussion was coordinated by V.F., F.S. and M.H.T. together with S.K.B. and H.L.; wavelet spectral analysis was performed by W.D. in collaboration with M.H.T.; paleoanthropological and archeological discussion and interpretation was done by F.S., R.V. and R.T.; R.T. provided expertise on evolutionary genetics, R.V. provided archeological context; data were provided by A.A. (catchment geology), V.F. (core stratigraphy, ICD and mineral composition); the manuscript was written by F.S., all authors contributed to the discussion and interpretation of the data and provided comments and suggestions to the manuscript.

Competing interests

The authors declare no competing interests.

Additional information

Supplementary information The online version contains supplementary material available at <https://doi.org/10.1038/s43247-021-00195-7>.

Correspondence and requests for materials should be addressed to F.S.

Peer review information *Communications Earth & Environment* thanks the anonymous reviewers for their contribution to the peer review of this work. Primary handling editor: Heike Langenberg.

Reprints and permission information is available at <http://www.nature.com/reprints>

Publisher's note Springer Nature remains neutral with regard to jurisdictional claims in published maps and institutional affiliations.



Open Access This article is licensed under a Creative Commons Attribution 4.0 International License, which permits use, sharing, adaptation, distribution and reproduction in any medium or format, as long as you give appropriate credit to the original author(s) and the source, provide a link to the Creative Commons license, and indicate if changes were made. The images or other third party material in this article are included in the article's Creative Commons license, unless indicated otherwise in a credit line to the material. If material is not included in the article's Creative Commons license and your intended use is not permitted by statutory regulation or exceeds the permitted use, you will need to obtain permission directly from the copyright holder. To view a copy of this license, visit <http://creativecommons.org/licenses/by/4.0/>.

© The Author(s) 2021